Interlayer Silylation of Layered Octosilicate with Organoalkoxysilanes: Effects of Tetrabutylammonium Fluoride as a Catalyst and the Functional Groups of Silanes

Masashi Yatomi, Masakazu Koike, Nadège Rey, Yuki Murakami, Shohei Saito, Hiroaki Wada, Atsushi Shimojima, David Portehault, Sophie Carenco, Clément Sanchez, et al.

Interlayer Silylation of Layered Octosilicate with Organoalkoxysilanes: Effects of Tetrabutylammonium Fluoride as a Catalyst and the Functional Groups of Silanes

Masashi Yatomi[+,[a]] Masakazu Koike[+,[a]] Nadège Rey,[b, c] Yuki Murakami,[a] Shohei Saito,[a] Hiroaki Wada,[a] Atsushi Shimojima,[a, d] David Portehault,[c] Sophie Carenco,[c] Clément Sanchez,[c] Carole Carcel,[b] Michel Wong Chi Man,*[b] and Kazuyuki Kuroda*[a, d]

Interlayer silylation of layered sodium octosilicate (Na-Oct) with various organoalkoxysilanes was conducted using hexadecyltrimethylammonium ion-exchanged layered octosilicate (C_{16}TMA-Oct) as an intermediate in the presence or absence of tetrabutylammonium fluoride (TBAF). The degree of silylation was increased by adding TBAF. It is suggested that F^- ions perform a nucleophilic attack on the alkoxysilanes, which promotes the silylation reaction. C_{16}TMA-Oct was silylated with octyltriethoxysilane (C_8TES) or 3-mercaptopropyltriethoxysilane (MPTES) to compare the reactivity of the two organoalkoxysilanes in the presence or absence of TBAF. A higher degree of silylation of C_{16}TMA-Oct was observed with MPTES, suggesting the higher accessibility of this silylating agent into the interlayer polar region of C_{16}TMA-Oct. Overall TBAF appears as a relevant catalyst for the covalent interlayer surface modification of layered silicates with organic functional groups.

Introduction

Layered silicates, composed of 2D crystalline silicate layers, are promising inorganic materials with high versatility in terms of design.[1–6] They possess interlayer exchangeable cations and reactive SiO^-/SiOH groups. The ion-exchange property and reactivity of the interlayer surfaces provide a variety of silica-organic hybrid materials that can find various applications, such as ion exchange, adsorption, and catalysis.[1,7–9] The effective use of interlayer space is also important for designing layered silicates as 2D nanomaterials.[1,10,11] The interlayer modification of layered silicates with silane coupling agents (silylating agents) is a practical method for increasing the chemical functionality of layered silicates. Indeed, various functional groups can be regularly grafted onto the surfaces of layered silicates by interlayer modification. Furthermore, this method enables the possibility to implement catalytic active sites, polymer growth sites, and porosity to layered silicates.[12–16] Thus, the regular interlayer modification of layered silicates with organic groups can maximize the advantages of silica-organic hybridization.[3]

We have developed the silylation of layered octosilicate, one of the layered silicates.[1] Layered octosilicate (Na-Oct (RUB-18): $Na_8[Si_{32}O_{64}(OH)_8]\cdot 32H_2O$)[17] possesses a pair of SiO^-/SiOH groups on the layer surfaces, as shown in Scheme 1a and Scheme 1b. In addition, the interlayer of octosilicate can be

[a] *M. Yatomi,[+] Dr. M. Koike,[+] Y. Murakami, Dr. S. Saito, Prof. Dr. H. Wada, Prof. Dr. A. Shimojima, Prof. Dr. K. Kuroda*
Department of Applied Chemistry, Faculty of Science and Engineering, Waseda University
3-4-1 Ohkubo, Shinjuku-ku, Tokyo 169-8555, Japan
E-mail: kuroda@waseda.jp

[b] *Dr. N. Rey, Dr. C. Carcel, Dr. M. Wong Chi Man*
Univ Montpellier, CNRS, ENSCM, 8 rue de l'école normale, 34290 Montpellier Cedex 5 (France)
E-mail: michel.wong-chi-man@enscm.fr

[c] *Dr. N. Rey, Dr. D. Portehault, Dr. S. Carenco, Prof. Dr. C. Sanchez Sorbonne Université, CNRS, Collège de France*
Laboratoire de Chimie de la Matière Condensée de Paris (CMCP)
4 place Jussieu, 75005, Paris, France

[d] *Prof. Dr. A. Shimojima, Prof. Dr. K. Kuroda*
Kagami Memorial Research Institute for Materials Science and Technology, Waseda University
2-8-26 Nishiwaseda, Shinjuku-ku, Tokyo 169-0051, Japan

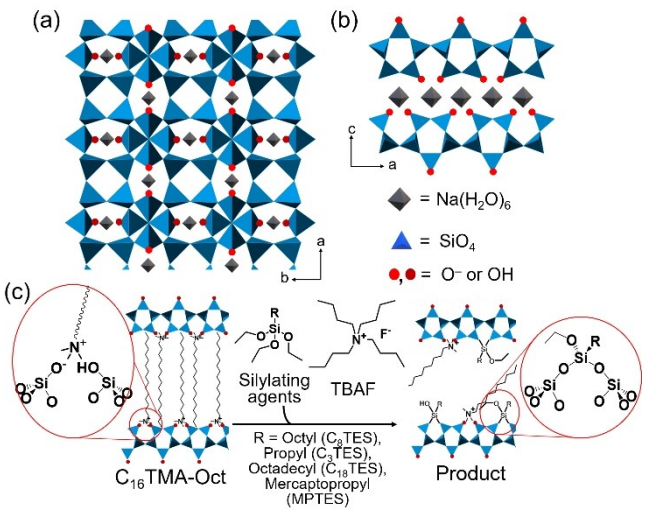

Scheme 1. (a) In-plane and (b) stacked structures of Na-Oct, and (c) dipodal silylation of C_{16}TMA-Oct.

expanded by the introduction of organic species, such as alkyltrimethylammonium cations, between the layers. These expanded octosilicate can subsequently be reacted with di- or tri-functional organosilylating agents dipodally (bidentate silylation), resulting in the formation of silica-organic hybrid compounds with an ordered arrangement of organic groups.[1]

Organochlorosilanes and organoalkoxysilanes are two major silylating agents for layered silicates. Organochlorosilanes are highly reactive; they react with sufficiently high yield with SiOH groups on the surfaces of silicate layers, affording a dense modification of the interlayer surfaces. However, the types of organic groups of organochlorosilanes are limited owing to the high reactivity of the Si–Cl bond towards organic functional groups. Furthermore, the generation of HCl produced by the reaction of chlorosilanes with silanol groups makes the reaction hard to control,[10,18] though this side effect is often reduced by using an HCl trapping agent (e.g., pyridine). In contrast, there is a greater variety of alkoxysilanes, and a wider range of organic modifications is possible. However, their reactivity towards silylation compared with organochlorosilanes is much lower. Therefore, the reactivity of organoalkoxysilanes for the silylation of silica and silicates must be substantially improved. The crucial factors affecting silylation reactions of layered silicates are thought to be the amount of silylating agent and the interlayer expansion with some intercalated species. Although these factors have been determined empirically from only few case studies,[18–20] a catalyst has scarcely been used for the silylation of layered silicates with organoalkoxysilanes. Kwon et al. reported the organosilylation of magadiite with octyltriethoxysilane[21] and that of kenyaite with 3-aminopropyltriethoxysilane[22] using a mixture of dodecylamine and ethanol. Although the catalytic action of dodecylamine was suggested, no details on the reaction mechanism were presented.

In this study, the effect of tetrabutylammonium fluoride (TBAF) on the silylation reactions of layered octosilicate with various organotriethoxysilanes (octyltriethoxysilane (C_8TES), propyltriethoxysilane (C_3TES), octadecyltriethoxysilane (C_{18}TES), and 3-mercaptopropyltriethoxysilane (MPTES)) was investigated (Scheme 1c and Table 1). TBAF is often used as a catalyst of sol-gel reactions namely to favor condensation of alkoxysilanes. Indeed, the fluoride ion of TBAF attacks the Si atom of alkoxysilanes, forming hypervalent silicon intermediates, which increases the nucleophilicity of Si and hence the reactivity.[23–26] Here we found that the degree of silylation of layered silicate using C_8TES was increased in the presence of TBAF for the first time. The catalytic effect of TBAF on the silylation reaction was verified with other organoalkoxysilanes, confirming the superiority of this method. The accessibility of organosilylating agents between layers strongly influenced the degree of silylation of layered silicates with or without TBAF. Interestingly, the addition of TBAF was found to improve the degree of silylation for less accessible silylating agents.

Results and Discussion

Effect of the presence of TBAF on the silylation of layered octosilicate with C_8TES

C_8TES presenting a medium-length alkyl chain was used as a model compound to investigate the effect of the addition of TBAF on the degree of silylation. Figure 1a-c shows the powder X-Ray diffraction (XRD) patterns of C_{16}TMA-Oct, C_8-Oct, and C_8-Oct_0.27F. The diffraction peak at $2\theta = 49°$, attributable to the (400) plane of the layered silicate structure, was observed for all the samples, indicating the retention of the crystal structure of octosilicate.[10] The profile of C_8-Oct obtained in the absence of TBAF (Figure 1b) shows that the basal spacing ($d = 2.47$ nm) decreased from that of the starting compound, C_{16}TMA-Oct ($d = 2.79$ nm, Figure 1a). When C_{16}TMA-Oct was modified with C_8TES in the presence of TBAF, the basal spacing was further reduced to $d = 2.23$ nm, as shown in Figure 1c. This decrease in basal spacing is consistent with the decrease in the amount of remaining C_{16}TMA in the sample obtained in the presence of TBAF, as determined from the elemental analysis and ^{13}C CP/MAS NMR data reported below.

Figure 2a–c shows the ^{29}Si MAS NMR spectra of C_{16}TMA-Oct, C_8-Oct, and C_8-Oct_0.27F. The ^{29}Si MAS NMR spectrum of C_{16}TMA-Oct (Figure 2a) shows the signals attributable to Q^3 (**Si**$(OSi)_3OH/O^-$) and Q^4 (**Si**$(OSi)_4$) units at -100 ppm and -111 ppm, respectively, with an integral intensity ratio of 1:1. These chemical shifts and peak intensities are consistent with those reported in previous studies.[7,9,10,17] The spectrum of C_8-Oct (Figure 2b) shows the signals arising from T^2 (C_8H_{17}**Si**-

Table 1. Experimental conditions.

Sample name	Silylating agent	Solvent	Reaction temp. [°C]	Reaction time / [d]	Molar ratio SiOH/SiO$^-$ [a]	Silylating agent	TBAF
C_8-Oct	Octyltriethoxysilane	DMF	100	4	1	10	0
C_8-Oct_0.027F	Octyltriethoxysilane	DMF	100	4	1	10	0.027
C_8-Oct_0.27F	Octyltriethoxysilane	DMF	100	4	1	10	0.27
C_8-Oct_0.54F	Octyltriethoxysilane	DMF	100	4	1	10	0.54
C_3-Oct	Propyltriethoxysilane	DMF	100	4	1	10	0
C_3-Oct_0.27F	Propyltriethoxysilane	DMF	100	4	1	10	0.27
C_{18}-Oct	Octadecyltriethoxysilane	Toluene	80	4	1	10	0
C_{18}-Oct_0.27F	Octadecyltriethoxysilane	Toluene	80	4	1	10	0.27
MP-Oct	3-mercaptopropyltriethoxysilane	DMF	100	4	1	10	0
MP-Oct_0.27F	3-mercaptopropyltriethoxysilane	DMF	100	4	1	10	0.27

[a] A pair of SiOH/SiO$^-$ of C_{16}TMA-Oct corresponds to one reaction site because of dipodal silylation.

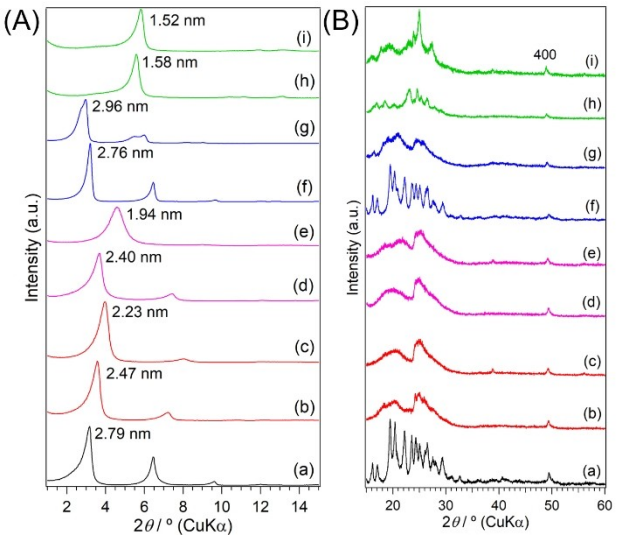

Figure 1. Powder XRD patterns of (a) C_{16}TMA-Oct, (b) C_8-Oct, (c) C_8-Oct_0.27F, (d) C_3-Oct, (e) C_3-Oct_0.27F, (f) C_{18}-Oct, (g) C_{18}-Oct_0.27F, (h) MP-Oct, and (i) MP-Oct_0.27F. **(A)** Profiles in the low angle region and **(B)** profiles with magnified intensities in the high angle region.

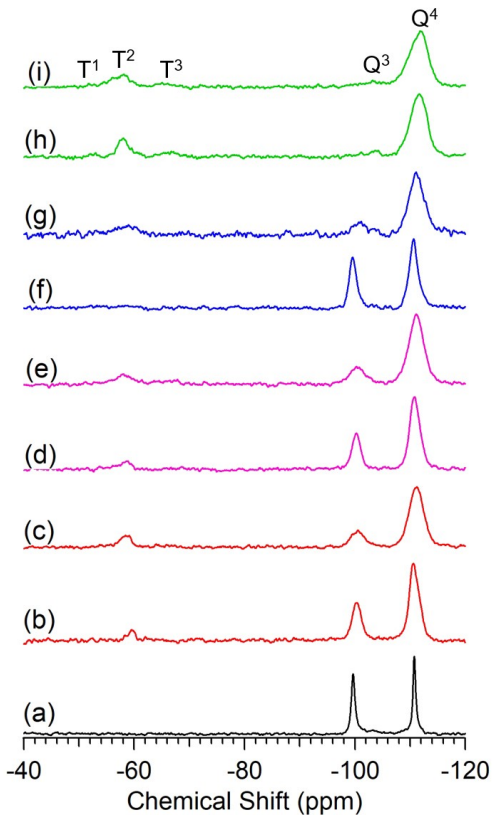

Figure 2. ^{29}Si MAS NMR spectra of (a) C_{16}TMA-Oct, (b) C_8-Oct, and (c) C_8-Oct_0.27F, (d) C_3-Oct, (e) C_3-Oct_0.27F, (f) C_{18}-Oct, (g) C_{18}-Oct_0.27F, (h) MP-Oct, and (i) MP-Oct_0.27F.

$(OSi)_2OH/OEt$), Q^3, and Q^4 units at the integral intensity ratio of 0.18:0.67:1.33 (Table S1). Because the Q^3 unit is converted to Q^4 by the silylation reaction and a T^2 environment appears, the degree of silylation of C_8-Oct (the ratio of the modified silylating agent to all the reaction sites on the octosilicate surfaces; one pair of $SiOH/SiO^-$ corresponding to one reaction site) was calculated to be 33% (($(1–Q^3) \times 100$). The spectrum of C_8-Oct_0.27F (Figure 2c) displays the signals arising from the T^2, Q^3, and Q^4 units at an integration ratio of 0.26:0.40:1.60 (Table S1). The degree of silylation, calculated in the same manner, was 60%. The broadening of the signal due to Q^4 (Figure 2c) is consistent with the increased formation of new Q^4 silicons by enhanced silylation. In addition, the ratios of the T^2 units to the decreases in the Q^3 units ($T^2/(1–Q^3)$) were approximately 1:2 for both of samples after silylation, suggesting dipodal silylation of the octosilicate surfaces.

Figure 3a–c shows the ^{13}C CP/MAS NMR spectra of C_{16}TMA-Oct, C_8-Oct, and C_8-Oct_0.27F; more details (enlarged profiles and peak assignments) are provided in Figure S1(A). When C_{16}TMA-Oct was modified with C_8TES with and without the addition of TBAF, a broad signal at 12.8 ppm attributable to $Si–CH_2$ (C′1), signals at 33.0 ppm, 30.4 ppm, and 23.6 ppm attributable to methylene groups ((C′3, C′6), (C′4, C′5), and (C′2, C′7), respectively) of octylsilyl group, and signals at 19.0 ppm and 59.7 ppm attributable to the methyl and methylene groups of ethoxysilyl group appeared in the spectra of both C_8-Oct and C_8-Oct_0.27F. In particular, the signals of the octylsilyl and ethoxysilyl groups are more intense in the spectrum of C_8-Oct_0.27F, indicating the idea that the addition of TBAF improves

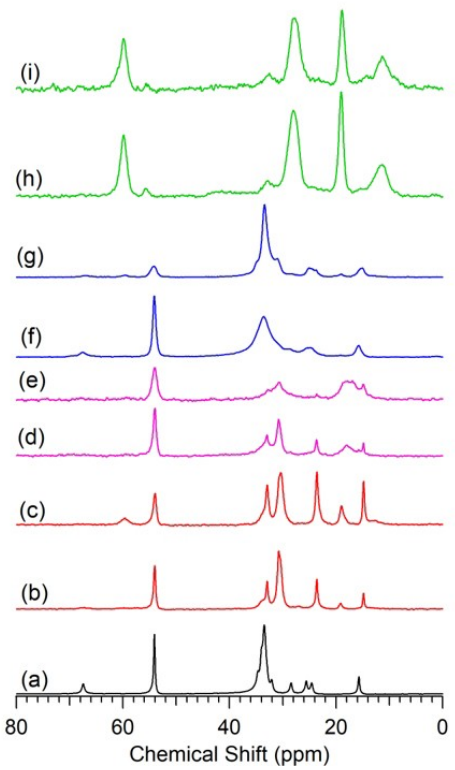

Figure 3. ^{13}C CP/MAS NMR spectra of (a) C_{16}TMA-Oct, (b) C_8-Oct, (c) C_8-Oct_0.27F, (d) C_3-Oct, (e) C_3-Oct_0.27F, (f) C_{18}-Oct, (g) C_{18}-Oct_0.27F, (h) MP-Oct, and (i) MP-Oct_0.27F.

the silylation yield. The enlarged profiles of C_{16}TMA-Oct, C_8-Oct, and C_8-Oct_0.27F (Figure S1(B) a–c) show that the signal at 33.5 ppm, attributable to the methylene group (C5 to C13) of the all-*trans* alkyl chain (Figure S1(B)a), shifts to 30.7 ppm (Figure S1(B)b and c), indicating the disordering in the all-*trans* methylene chain of the remaining C_{16}TMA.[27] The FT-IR spectrum of C_{16}TMA-Oct (Figure S2a, SI) indicates the presence of a band at 3030 cm^{-1}, attributable to the C–H stretching vibration of the NCH_3 group, the bands at 2919 cm^{-1} and 2850 cm^{-1}, attributable to the asymmetric and symmetric C–H stretching of CH_2, and the peaks at 2950 cm^{-1} and 2870 cm^{-1}, attributable to the asymmetric and symmetric C–H stretching of the terminal CH_3 group of the alkyl chain, respectively.[28] The FT-IR spectra of both C_8-Oct and C_8-Oct_0.27F indicate that the intensities of these bands were weakened (Figure S2b and c, SI), which is consistent with the ^{13}C CP/MAS NMR results.[29] In addition, the intensity of the band at 960 cm^{-1} due to the Si–OH stretching vibration of the silanol group[16,30] decreased, which also indicates the introduction of the octylethoxysilyl group, as schematically shown in the diagram of the dipodal grafting in Scheme 1; however, the difference in the degree of decrease between C_8-Oct and C_8-Oct_0.27F is not so clear from the FT-IR data.

The elemental analysis of the samples (Table S2) also support the above results. The amount of nitrogen was reduced from 2.4 wt% of C_{16}TMA-Oct to 1.5 wt% and 1.0 wt% for C_8-Oct and C_8-Oct_0.27F, respectively, due to the grafting of C_8TES. Because the observed contents of nitrogen were relatively low (1.0 wt% and 1.5 wt%), the calculated values presented here should be treated as semi-quantitative estimates. By multiplying each Si content (18.7 wt%, 21.9 wt%, and 24.6 wt%) by the ^{29}Si MAS NMR intensity ratio $(Q^3+Q^4)/(T^2+Q^3+Q^4)$ (1.00, 0.92, and 0.88, respectively), the octosilicate-derived content Si(Si(Q)) was calculated to be 18.7 wt%, 20.0 wt%, and 21.8 wt% for C_{16}TMA-Oct, C_8-Oct, and C_8-Oct_0.27F, respectively. Accordingly, the N/Si(Q) ratios for C_{16}TMA-Oct, C_8-Oct, and C_8-Oct_0.27F were 0.26, 0.15, and 0.09, respectively, suggesting that the C_{16}TMA cations were desorbed. The amounts of carbon arising from C_8TES in C_8-Oct and C_8-Oct_0.27F were 5.5 wt% and 12.5 wt%, respectively.[31] The ratio of C_8TES-derived C to Si(Q) content (C(C_8TES)/Si(Q)) was calculated to be 0.64 and 1.34, indicating that the degree of silylation of layered octosilicate with C_8TES is significantly improved by the catalytic amounts of TBAF.

Effect of the amount of TBAF on the silylation with C_8TES and plausible silylation reaction mechanism

The powder XRD patterns of C_8-Oct and C_8-Oct_*x*F ($x=0.027$, 0.27, or 0.54) are shown in Figure S3. The diffraction peak at $2\theta=49^\circ$ was observed for all the samples, suggesting the retention of the crystallinity in the in-plane direction.[10] The *d* values of the basal spacing gradually decreased ($d=2.47$ nm→2.39 nm→2.26 nm→2.23 nm) with the increase in the amount of TBAF added. The CHN analysis and solid-state ^{13}C NMR data of the samples, as described later, show that the amount of C_{16}TMA continuously decreased with the increasing amount of TBAF. Consequently, the decrease in the basal spacing indicates the progress of the desorption of C_{16}TMA cations, which is consistent with the above-mentioned results.

The ^{29}Si MAS NMR spectra of C_8-Oct and C_8-Oct_*x*F are shown in Figure S4. The Q^3 and Q^4 signals were observed at −100 ppm and −111 ppm, respectively, for both C_8-Oct_0.027F and C_8-Oct_0.54F, which are consistent with those of C_8-Oct_0.27F mentioned in the section above. The degrees of silylation calculated from the integral intensity ratios of the signals were 54%, 60%, and 71% for C_8-Oct_0.027F, C_8-Oct_0.27F, and C_8-Oct_0.54F, respectively (Table S1). This indicates that the silylation reactivity of layered octosilicate with C_8TES is enhanced with increasing amounts of TBAF. Only the T^2 peak appeared as a signal arising from C_8TES in the spectrum of C_8-Oct_0.027F. The ratio of the T^2 signal intensity over the reduced intensity in the Q^3 signals before and after the silylation was 1:2, which supports the observation that the dipodal silylation proceeds in a manner similar to that of C_8-Oct_0.27F. In addition, the amount of the added catalyst corresponds to 2.7% of the reaction sites of layered octosilicate, but the degree of silylation proceeds by 21%, which suggests that F^- acts as a catalyst. On the other hand, both T^2 and T^3 (R**Si**$(OSi)_3$) signals were observed for C_8-Oct_0.54F. This is probably due to the condensation between proximal silylating agents by hydrolysis and condensation of ethoxy groups because the amount of water increased with increasing amount of added TBAF (knowing that TBAF contains 5.7 wt% water, as stated in the Materials in the Experimental Section).

Figure S5 shows the ^{13}C CP/MAS NMR spectra of C_8-Oct and C_8-Oct_*x*F. The relative intensity ratio of the signal at 54.1 ppm, attributed to N–CH_3 of C_{16}TMA cations over the other signals due to the octyl group,[27] decreased with increasing amount of TBAF. The relative intensity ratio of the broad signal at 12.8 ppm, attributed to Si–CH_2, the signals at 19.0 ppm and 59.7 ppm, attributed to the methyl and methylene groups of the ethoxysilyl group, and the signal at 23.6 ppm, attributed to the methylene group (C′2, C′7) of octylsilyl group, also increased with increasing amounts of TBAF by comparison with the intensity of the signals due to C_{16}TMA cations.

The contents of nitrogen gradually decreased (1.5 wt%→1.1 wt%→1.0 wt%→0.8 wt%) with increasing amounts of TBAF added, while the carbon content arising from C_8TES, calculated by subtracting the amount of carbon arising from $C_{16}TMA^+$, gradually increased (5.4 wt%→11.8 wt%→12.5 wt%→17.4 wt%). The value of N/Si(Q) decreased from 0.15 to 0.10, 0.09, and finally 0.09, and the ratio of C(C_8TES)/Si(Q) increased from 0.63 to 1.26, 1.34, and finally 2.06. These results also show that increasing amounts of TBAF results in increasing amounts of eliminated C_{16}TMA cations and introduced octylethoxysilyl groups.

The mechanism of the silylation without the addition of fluoride ions can be explained as follows. The reaction was conducted at 100 °C, and EtOH was generated each time alkoxysilane reacted with SiOH, accompanied by the generation of water by the reaction of EtOH with surface silanol groups.[13,32,33] Consequently, C_{16}TMA cations may be eliminated as hydroxide.[13] Here, we discuss the reaction mechanism of the

promotion of silylation by the addition of fluoride ion (TBAF) on the basis of the sol-gel reaction of alkoxysilanes catalyzed by fluoride ions (Scheme 2).[23–26]

A) An XPS peak[34] due to the F 1s orbital at 687 eV, attributed to the Si–F bond,[35] was observed (Figure S6), indicating the formation of unidentified Si species with an Si–F bond; this, in turn, indicates the nucleophilic attack on the silylating agent.[36]

B) It is plausible that the oxygen atom of the Si–OH group at the surfaces of the layers undergoes nucleophilic attack on the Si atom that has become electrophilic due to the formation of Si–F bonds, resulting in the formation of a hexacoordinated state with Si–O–Si.

C) Then, a tetracoordinated state can form by the elimination of EtOH and F^- from the hexacoordinated silicon; this process generally occurs in sol-gel reactions catalyzed by fluoride ions. Then, the silylation is completed by processes D) to G), as in the case where there are no fluoride ions.

Silylation of C_{16}TMA-Oct with silylating agents having different alkyl chain lengths

To investigate the effect of the alkyl chain length of silylating agents on the degree of silylation, reactions using C_3TES and C_{18}TES were conducted to compare the results with those obtained using C_8TES. Hereafter, the ratio of TBAF per the reaction site of layered octosilicate was fixed at 0.27 because T^3 units, showing unfavorable condensation between organoalkoxysilanes, appeared for the case of C_8-Oct_0.54F.

Figure 1d–g shows powder XRD patterns of C_3-Oct, C_3-Oct_0.27F, C_{18}-Oct, and C_{18}-Oct_0.27F. As described above, the diffraction peak at $2\theta = 49°$, attributed to the in-plane (400) plane of the octosilicate,[10] was observed for all the samples. When C_3TES was used as the silylating agent, as shown in the profiles of Figure 1d and Figure 1e, the basal spacing decreased from $d = 2.79$ nm for C_{16}TMA-Oct to $d = 2.40$ nm (C_3-Oct) and 1.94 nm (C_3-Oct_0.27F), respectively. The gallery heights (1.66 and 1.20 nm for C_3-Oct and C_3-Oct_0.27F, respectively), which were calculated by subtracting the layer thickness (0.74 nm)[37] from the basal spacings, do not correspond to the length of propyl group (0.37 nm) grafted on the layers, which suggests partial removal of C_{16}TMA cations, as supported by the decrease in the amount of nitrogen (described below). When C_{18}TES was modified (Figure 1f and Figure 1g), the basal spacings were $d =$ 2.76 nm and 2.96 nm for C_{18}-Oct and C_{18}-Oct_0.27F, respectively. The larger d value of the basal spacing of C_{18}-Oct_0.27F compared to that of C_{16}TMA-Oct suggests the introduction of C_{18}TES owing to the longer alkyl chain of C_{18}TES compared to that of the C_{16}TMA cation. On the other hand, the basal spacing of C_{18}-Oct remained similar to that of C_{16}TMA-Oct, suggesting that the amount of grafted silylating agent between layers was small, as supported by the ^{29}Si MAS NMR data described below.

Interestingly, there is a linear relationship between the number of carbon atoms in the alkyl chain and the d value of the basal spacing (Figure 4). The increase in the basal spacing

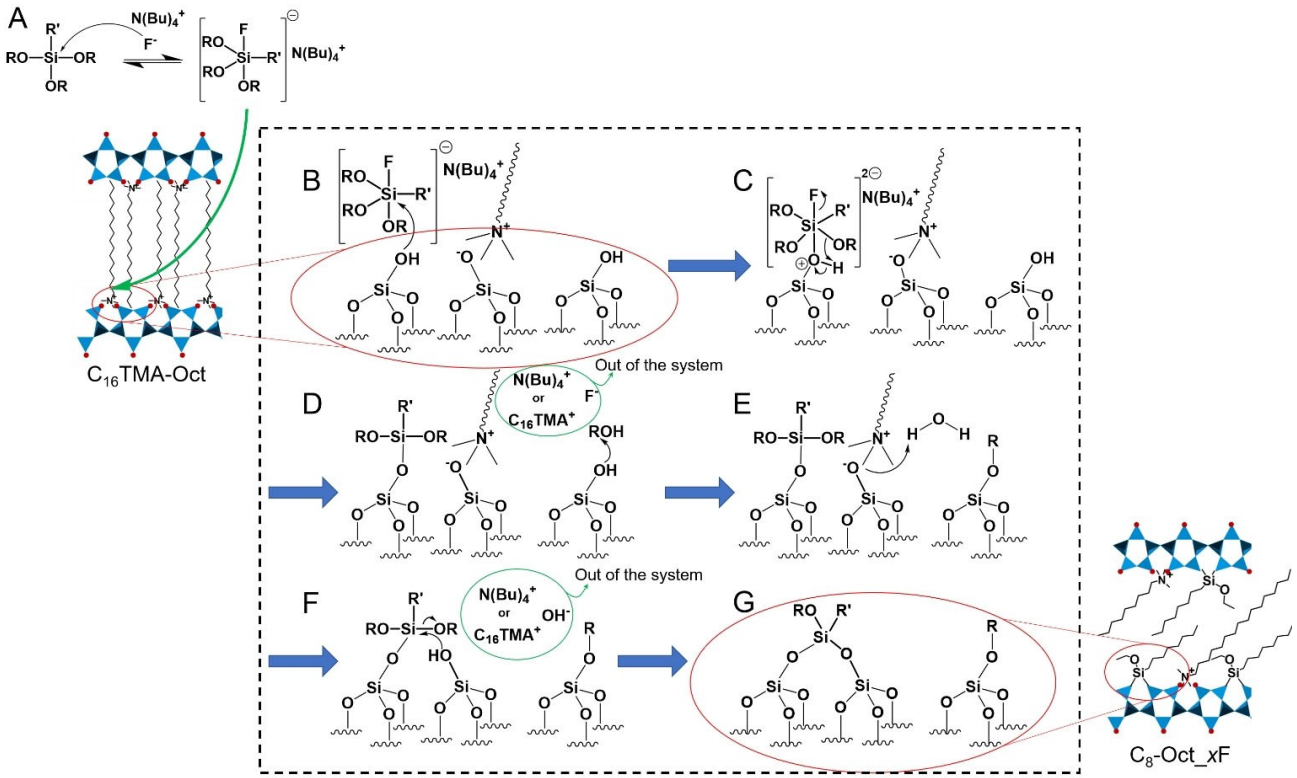

Scheme 2. Plausible reaction mechanism of silylation of layer surfaces of layered octosilicate by the addition of fluoride ions.

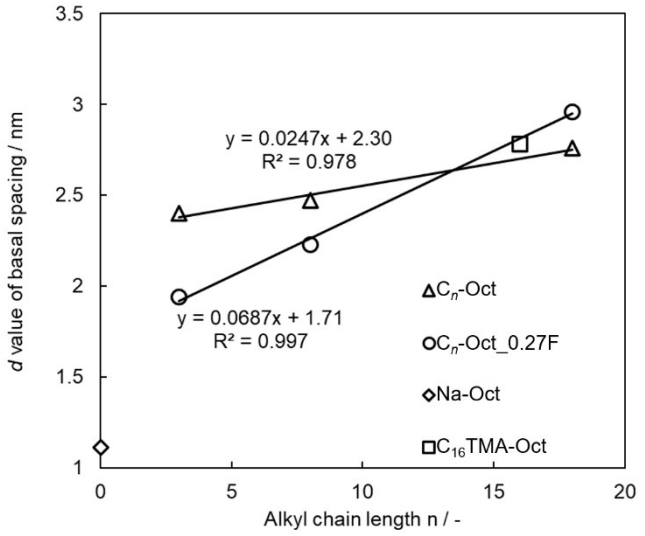

Figure 4. Relationships between the number of carbon atoms in alkyl chain and *d* values of basal spacing of C_n-Oct and C_n-Oct_0.27F.

per CH_2 of the silylating agent was 0.0247 and 0.0687 nm for the three samples prepared without and with TBAF, respectively. Note that the R^2 values, i.e., the degree of data dispersion, are close to 1. In general, the increase per CH_2 in the length of the all-*trans* alkyl chain is calculated to be 0.125 nm (0.154 nm (C–C bond length) × sin(54.75°)). The increase of 0.125 nm per CH_2 unit indicates a monolayer arrangement of alkyl groups oriented perpendicular to the layer. If the increase is twice the value, the arrangement should be bilayered perpendicularly to the layers. The observed data are much smaller than the values calculated from the perpendicularly oriented alkyl chain lengths of silylating agents. Accordingly, the relatively small inclination of the relationships between the basal spacings and the carbon chain lengths (Figure 4) for all the samples should be influenced by tilted alkyl groups on silyl groups to the layer and the co-presence of remaining C_{16}TMA cations between the layers. The inclination of the line for the samples prepared without TBAF is smaller than that prepared with TBAF, which is in accordance with the lower amounts of eliminated C_{16}TMA ions in the samples prepared without TBAF, as described below.

Figure 2d–g shows the ^{29}Si MAS NMR spectra of C_3-Oct, C_3-Oct_0.27F, C_{18}-Oct, and C_{18}-Oct_0.27F. The degree of silylation using C_3TES was calculated to be 41% and 59% for the samples prepared with and without TBAF, respectively (see Table S1 for the details of calculation). Similarly, the degree of silylation with C_{18}TES was 23% and 68%, respectively (see Table S1 for the details of calculation). The degree of silylation of C_{18}-Oct without the addition of TBAF was lower than those of C_8-Oct and C_3-Oct. The solvent for the reaction using C_{18}TES was changed from DMF to toluene because C_{18}TES does not dissolve in DMF. Because C_{16}TMA-Oct does not swell as much in toluene, it is likely that C_{18}TES, which is longer than C_{16}TMA, has lower accessibility to the interlayer spaces, which reduces the degree of silylation. However, our preliminary study on the use of toluene for the C_8TES case showed that the difference in the silylation reactivities was not large (data not shown).

The degree of silylation was higher for the silylating agents with shorter alkyl chains (C_3-Oct: 41%, C_8-Oct: 33%, C_{18}-Oct: 23%) when TBAF was not added. This can be explained by the accessibility of the silylating agent between the layers. It was also confirmed that the addition of TBAF improves the degree of silylation for all the cases using a silylating agent with an alkyl chain (Table S1). In particular, the degree of silylation was significantly improved for the case of C_{18}-Oct_0.27F, which is in good agreement with Scheme 2, showing that the added TBAF contributes to the increase in the reactivity of the organotrieth-oxysilyl group. This should be effective in overcoming the limitation of the accessibility of the silylating agent between layers.

Figure 3d–g shows the ^{13}C CP/MAS NMR spectra of C_3-Oct, C_3-Oct_0.27F, C_{18}-Oct, and C_{18}-Oct_0.27F. These results indicate the introduction of the respective silylating agents and the partial elimination of C_{16}TMA cations. More details can be found in the Supporting Information (page S10). As in the case of C_8TES, the amounts of the silylating agents introduced were increased by the presence of TBAF, and the amounts of C_{16}TMA cations decreased accordingly (see Table S2 for details). These results support the increase in the degree of silylation with C_3TES and C_{18}TES by the addition of TBAF.

Effect of the mercapto group of the silylating agent on the degree of silylation

C_{16}TMA-Oct was silylated with MPTES possessing a mercapto (thiol) group that can be developed for further applications. Compared to the case when using alkyltriethoxysilanes, the degree of silylation was very high when using MPTES with or without TBAF (Table S1). Below, we discuss the factors that play an important role in the silylation of C_{16}TMA-Oct.

Figure 1h and Figure 1i shows the powder XRD patterns of MP-Oct and MP-Oct_0.27F. The basal spacings were $d = 1.52$ nm (MP-Oct) and 1.58 nm (MP-Oct_0.27F). The relatively large amount of introduced silyl groups and the small amount of residual C_{16}TMA ions, as described below, can explain the relatively small basal spacings of the products using MPTES, when compared with the cases using C_3TES. A lamellar structure with mercaptopropyl groups bonded onto the siloxane layer can be fabricated by hydrolysis and condensation of α, ω-bis (trimethoxysilyl)propyldisulfide and the subsequent reduction of the disulfide bond.[38] However, the *d* value in the stacking direction of the lamellar phase was about 1.2 nm and the value is different from those of MP-Oct and MP-Oct_0.27F because the two samples have thicker octosilicate layers.

Figure 2h and Figure 2i shows the ^{29}Si MAS NMR spectra of MP-Oct and MP-Oct_0.27F. The degree of silylation of MP-Oct and MP-Oct_0.27F was calculated to be 89% and 80%, respectively (Table S1), indicating a higher degree of silylation even in the case of MPTES without the addition of TBAF. Figure 3h and. Figure 3i shows the ^{13}C CP/MAS NMR spectra of

MP-Oct and MP-Oct_0.27F, respectively. In these spectra, a relatively large decrease in the signal attributed to N–CH_3 at 54.1 ppm was observed, suggesting a significant elimination of C_{16}TMA cations. The introduction of 3-mercaptopropylethoxysilyl groups was also confirmed, and the detailed assignments of the ^{13}C NMR signals are shown in SI (page S10). The Raman spectra of MP-Oct and MP-Oct_0.27F (Figure S7) show peaks attributable to S–H stretching at 2570 cm^{-1}, confirming the presence of mercapto groups,[39,40] which supports the ^{13}C CP/MAS NMR results. A very small peak at 510 cm^{-1} was also observed, suggesting the formation of a disulfide bond.[41]

The N contents of MP-Oct and MP-Oct_0.27F were 0.0 wt% and 0.2 wt%, respectively. The amounts of carbon arising from MPTES in MP-Oct and MP-Oct_0.27F were 11.1 wt% and 9.1 wt%, respectively (Table S2).[42] The calculated amounts of carbon of MP-Oct and MP-Oct_0.27F based on the respective silylation rates (89% and 80%) were 12.7 wt% and 12.0 wt%, respectively, if all ethoxy groups remained after the dipodal silylation; when all ethoxysilyl groups were hydrolyzed to silanol groups, the carbon content was calculated to be 8.5 wt% and 7.9 wt%, respectively. In all cases, the measured values (11.1 wt% and 9.1 wt%) are within the range of these calculated values. Thus, some ethoxy groups in both samples should be eliminated. The contents of S of both samples were same as 7.1 wt% (Table S2). The equal amounts of S, despite the difference in the degree of silylation is probably due to the variation in the amount of ethoxy groups remaining after the silylation. The residual ratios of ethoxy groups were calculated to be approximately 60% for MP-Oct and approximately 20% for MP-Oct_0.27F from the C/S ratios (4.2 and 3.4, respectively).[43] Therefore, in both MP-Oct and MP-Oct_0.27F, the ethoxy groups were partially eliminated, and it was confirmed that the amounts of carbon and sulfur were within a reasonable range.

The reason why silylation of C_{16}TMA-Oct with MPTES proceeds in a higher degree than those with alkyltrialkoxysilanes (C_nTES, where C_n accounts for the number of carbon atoms in the alkyl chain (n = 3, 8, and 18)) is discussed here. Two possible differences between C_nTES and MPTES can be highlighted. (1) The first one is the fact that the electron density of Si of the silylating agents varies depending on the functional group,[44] which may affect the reactivity. However, in the following paragraph we show that this does not explain the high degree of silylation with MPTES. (2) The second difference between C_nTES and MPTES lies in the polar S–H groups of MPTES, which may provide a higher accessibility to polar reaction sites (organoammonium cations on Si–OH/Si–O^- groups) between layers than for C_nTES with non-polar alkyl groups.

The reason why point (1) above cannot account for the observed difference in silylation degree between MPTES and CnTES is shown below. The solution ^{29}Si NMR spectra of C_3TES and MPTES are shown in Figure S8. The signals due to the T^0 unit (R**Si**$(OEt)_3$) were observed for both spectra at the chemical shifts of −44.95 ppm for C_3TES and −45.88 ppm for MPTES.[45] The chemical shift of Si in C_3TES is located at a slightly lower magnetic field, indicating that Si in C_3TES has a lower electron density.[44] Therefore, C_3TES should be relatively more susceptible to nucleophilic attacks by silanol groups on the layer surfaces, and the degree of silylation should be higher. In practice, however, C_3TES had a lower degree of silylation. According to a report on the hydrolysis rates of alkyltrieth-oxysilanes by Echeverria *et al.*,[44] alkoxysilanes, in which the chemical shift of Si appears on the lower magnetic field owing to the difference in the functional groups of the alkyl moiety, have more electrophilic Si and consequently, higher hydrolysis rate of the alkoxysilanes. Therefore, it is suggested that the reaction rate of silylation using C_3TES is higher than that using MPTES. However, the actual high and low degrees of silylation were opposite to the expected trend. This is presumably because the reaction time was sufficiently long, and the relatively higher reaction rate did not affect the degree of silylation.

The reason why point (2) is a reasonable explanation is as follows. The silylation reaction of mesoporous silica SBA-15 composed of amorphous silica pore walls was performed. Since the surfactant used in the preparation of SBA-15 was removed by calcination, all the reaction sites are silanol groups. Figure 5 shows the ^{29}Si MAS NMR spectra of SBA-15, C_3-SBA, C_8-SBA, C_8-SBA_F, MP-SBA, and MP-SBA_F (the deconvoluted spectra are shown in Figure S9). In the spectrum of SBA-15 (Figure 5a), the signals assigned to the Q^2 (**Si**$(OSi)_2(OH)_2$), Q^3, and Q^4 units were observed at −90 ppm, −101 ppm, and −110 ppm, respectively; the integral intensity ratio of the three signals was 0.03 : 0.31 : 0.66. In the spectra of C_3-SBA and MP-SBA (Figure 5b and Figure 5e), the signals attributed to the Q^2, Q^3, and Q^4 units were observed at the same positions. The integral intensity

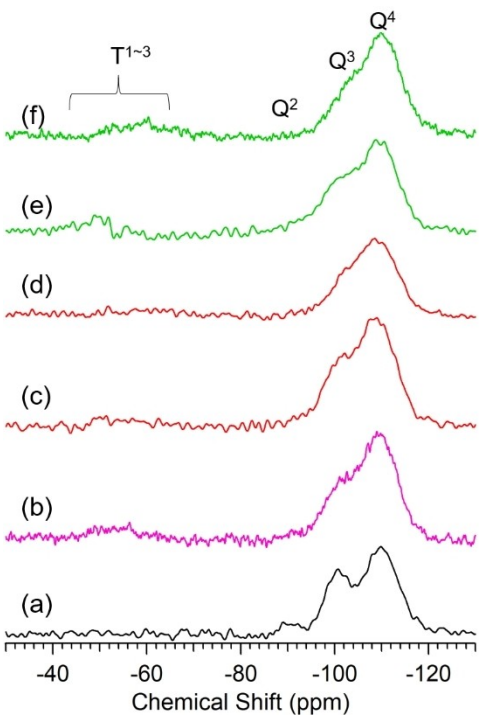

Figure 5. ^{29}Si MAS NMR spectra of (a) SBA-15, (b) C_3-SBA, (c) C_8-SBA, (d) C_8-SBA_F (e) MP-SBA, and (f) MP-SBA_F.

ratios (Q^2:Q^3:Q^4) were 0.02:0.31:0.67 for C_3-SBA and 0.03:0.27:0.70 for MP-SBA. The spectra of C_8-SBA, C_8-SBA_F, and MP-SBA_F (Figure 5c, Figure 5d, and Figure 5f) showed signals arising from Q^3 and Q^4 units at the integral intensity ratios of 0.30:0.70, 0.27:0.73, and 0.22:0.78, respectively. The degree of silylation of SBA-15 was calculated by a way different from that used for octosilicate. Owing to the presence of the Q^2 unit in SBA-15, the degree of silylation was estimated from the consumption of silanol groups. The ratios of the silanol groups consumed over the total contents of silanol groups were calculated to be 0.02, 0.07, 0.10, 0.04, and 0.15 for C_3-SBA, C_8-SBA, C_8-SBA_F, MP-SBA, and MP-SBA_F, respectively. These values are consistent with previously reported values observed for SBA-15 silylated with octadecyltrimethoxysilane.[46] The amounts of silanol groups consumed for the silylation was similar when using C_3-SBA, C_8-SBA, and MP-SBA, which was different from when layered octosilicate was used. This indicates that the reactivities and accessibility of C_3TES, C_8TES, and MPTES to the reaction sites on SBA-15 surfaces are similar, indicating that MPTES is more accessible than C_nTES in the ionically modified interlayer surfaces of layered octosilicate. Furthermore, the increase in the degree of silylation of SBA-15 with both C_8TES and MPTES with the addition of TBAF was also confirmed.

It is interesting to note that the morphologies of C_8-Oct_0.27F, C_3-Oct_0.27F, and C_{18}-Oct_0.27F were slightly different from that of MP-Oct_0.27F (Figure S10). In particular a slight disintegration of layers was observed for the former three samples (Figures S10a, b, and c) but not in MP-Oct_0.27F (Figure S10d). However, further analysis is difficult at this stage.

The higher degree of silylation of octosilicate with MPTES was observed even when TBAF was not added. Because there are no large differences in the reactivity of C_nTES and MPTES for the silylation onto SBA-15, the polarity of the mercapto group is likely to increase the accessibility to the interlayer surfaces of layered octosilicate where organoammonium cations are located.

Conclusion

The addition of TBAF was found to promote the interlayer silylation of layered octosilicate with C_8TES. The degree of silylation increased with an increase in the amount of TBAF added. When the ratio of TBAF to the reaction sites of silicate increased, the water content in the reaction system increased due to the presence of water in TBAF, which caused side reactions. The role of fluoride ions in the promotion of silylation was proposed. Although the degree of silylation using a silylating agent with different alkyl chains was improved by the addition of TBAF, MPTES improved the accessibility between layers due to its polarity, resulting in a higher degree of silylation without the addition of TBAF. The addition of TBAF in the silylation of a layered silicate effectively promoted the silylation of alkylalkoxysilanes with low interlayer accessibility. Because silica and silicates are diverse in structure and reactivity, the search for appropriate catalysts or suitable experimental conditions for the preparation of silica-organic hybrid materials by silylation will be further developed using the concept reported here.

Experimental Section

Materials

SiO_2 (fumed silica (S5130), Sigma Aldrich), NaOH (FUJIFILM Wako Pure Chemical Corp., 97%), hexadecyltrimethylammonium chloride (C_{16}TMACl, Tokyo Chemical Ind. Co., Ltd., 95%), octyltriethoxysilane (C_8TES, Tokyo Chemical Ind. Co., Ltd., 97%), propyltriethoxysilane (C_3TES, Tokyo Chemical Ind. Co., Ltd., 98%), octadecyltriethoxysilane (C_{18}TES, Tokyo Chemical Ind. Co., Ltd., 85%), 3-mercaptopropyltriethoxysilane (MPTES, Tokyo Chemical Ind. Co., Ltd., 96%), tetraethoxysilane (TEOS, Tokyo Chemical Industry Co., Ltd.), triblock copolymer EO20PO70EO20 (Pluronic 123, Sigma Aldrich), hydrochloric acid (6 M, FUJIFILM Wako Pure Chemical Corp.), super dehydrated *N, N*-dimethylformamide (DMF, FUJIFILM Wako Pure Chemical Corp., 99.5%), super dehydrated toluene (FUJIFILM Wako Pure Chemical Corp., 99.5%), acetone (Kanto Chemical Co., Inc., 99.0%), tetrabutylammonium fluoride in tetrahydrofuran (1.0 M TBAF in THF, Sigma Aldrich), and super dehydrated THF with stabilizer free (THF, FUJIFILM Wako Pure Chemical Corp., 99.5%) were used without further purification. The liquid state ^{1}H NMR spectrum of 1.0 M TBAF in THF showed the presence of 5.7 wt% water, which is consistent with the analysis conducted by Sigma Aldrich.

Mesoporous silica SBA-15 was prepared according to a previously reported method.[47,48] To investigate the effect of inorganic support on silylation, a silylation reaction was performed on mesoporous silica SBA-15 instead of layered octosilicate. Hydrochloric acid (0.6 M, 40 g), water (110 g), and surfactant (P123, 4 g) were mixed in an eggplant flask and the mixture was stirred until the P123 was dissolved. TEOS (8.5 g) was added to the mixture, and the resulting mixture was stirred at 45 °C for 8 h first and then at 80 °C for 15 min. The product was separated by filtration, washed with water, dried at room temperature, and then treated thermally at a rate of 1 °C/min and calcined at 550 °C for 6 h to obtain SBA-15. The synthesis was confirmed by powder XRD (Fe$K\alpha$), TEM, and SEM data (Figure S11–Figure S13, Supporting Information (SI)).

Preparation of Na-Oct and C_{16}TMA-Oct

Layered Na-octosilicate was synthesized according to a previously reported method with some modification.[37] SiO_2, NaOH, and deionized water were mixed at a ratio of 4:1:25.8. The mixture was hydrothermally treated in an autoclave at 100 °C for 4 weeks. The product was washed with deionized water three times, vacuum filtered with a filter paper (ADVANTEC 5 C), and dried at 45 °C to obtain Na-Oct. The formation of Na-Oct was confirmed by powder XRD, ICP-OES, and ^{29}Si MAS NMR data, shown in SI (Figure S14–Figure S16, Figure S18, and Table S3). C_{16}TMA-Oct was also obtained following the procedure reported previously.[10,37] Na-Oct (1.5 g) was dispersed in an aqueous solution of C_{16}TMACl (0.1 M, 100 mL); the mixture was stirred at room temperature for 24 h, and the supernatant was removed by centrifugation. This ion exchange step was repeated twice. Finally, the product was washed with deionized water twice and dried under reduced pressure at room temperature to obtain C_{16}TMA-Oct. The formation of C_{16}TMA-Oct was confirmed by powder XRD, ^{29}Si MAS NMR, FT-IR, ^{13}C CP/MAS NMR, SEM, ICP-OES, and CHN analysis; these data are shown in SI (Figure S14–Figure S18 and Table S3)

Silylation of C_{16}TMA-Oct

The reaction of C_{16}TMA-Oct with C_8TES as a silylating agent is described below as a typical example. C_{16}TMA-Oct (0.2 g) was dried in a Schlenk flask under reduced pressure at 120 °C for 2 h. Then, the sample was heated at 100 °C and the atmosphere was changed from air to dry N_2. After this treatment, DMF (4 mL), C_8TES (1.15 mL), and a THF solution of TBAF[49] (variable amounts) were added to C_{16}TMA-Oct and the mixture was stirred for 4 d (the reason for the selection of 4 d is described in the Supplementary Information, Figure S19). The amount of C_8TES was ten times greater than necessary for the quantitative capping of the reaction sites (SiOH/SiO^-) of C_{16}TMA-Oct supposing dipodal silylation with diethoxy groups. The amount of added TBAF in THF was varied from 0.1 mL of 0.1 M solution and 1 mL of 0.1 M solution to 0.2 mL of 1 M solution; these correspond to 0.027, 0.27, or 0.54, equivalent to the one reaction site of the layer surfaces of the octosilicate. After cooling to room temperature, the reaction product was centrifuged, washed with DMF and acetone, and further dried under reduced pressure. To investigate the effect of fluoride ions on the silylation reaction, a sample was prepared without adding a TBAF solution. The sample were names as follows: C_8-Oct (no TBAF added) and C_8-Oct_*x*F ($x = 0.027$, 0.27, or 0.54).

The effect of other silylating agents on the degree of silylation was also investigated. C_3TES (0.85 mL), C_{18}TES (1.76 mL), or MPTES (0.88 mL) was reacted with C_{16}TMA-Oct with a constant amount of TBAF ($x = 0.27$); these samples are denoted as C_3-Oct_0.27F, C_{18}-Oct_0.27F, and MP-Oct_0.27F, respectively. Samples without TBAF were also prepared (sample names: C_3-Oct, C_{18}-Oct, and MP-Oct). Because C_{18}TES is not soluble in DMF, silylation was performed in toluene at 80 °C.

Silylation of SBA-15

SBA-15 (0.1 g) was dried under reduced pressure at 120 °C for 2 h. Then, the sample was heated at 100 °C, and the atmosphere was changed from air to dry N_2. After this treatment, DMF (4 mL) and a silylating agent (C_3TES (0.85 mL), C_8TES (1.15 mL), or MPTES (0.88 mL)) were added to SBA-15, and the mixture was stirred for 4 d. After cooling to room temperature, the reaction product was centrifuged, washed with DMF and acetone, and further dried under reduced pressure. The samples silylated with C_3TES, C_8TES, and MPTES were denoted as C_3-SBA, C_8-SBA, and MP-SBA, respectively. Samples with a TBAF solution (0.1 M, 1 mL) and C_8TES or MPTES were also prepared and were denoted as C_8-SBA_F and MP-SBA_F, respectively.

Characterization

Powder X-ray diffraction (XRD) patterns were obtained by a parallel method using a Rigaku Ultima-III powder diffractometer (Cu Kα, $\lambda =$ 0.15418 nm, 40 kV, 40 mA) and a Rigaku Ultima IV diffractometer (Fe Kα, $\lambda = 0.19373$ nm, 40 kV, 30 mA). Solid-state ^{29}Si MAS NMR spectra were recorded on a JEOL ECX-400 spectrometer at a resonance frequency of 78.6 MHz, a recycle delay of 500 s, and a 90° pulse. Samples were packed in 4 mm zirconia sample tubes and spun at 6 kHz. Solid-state ^{13}C CP/MAS NMR spectra were recorded on a JEOL ECX-400 spectrometer at a resonance frequency of 99.55 MHz, recycle delay of 10 s, and contact time of 5 ms. Samples were packed in a 4 mm silicon nitride sample tube and spun at 6 kHz. Each chemical shift was corrected using −33.8 ppm of polydimethylsilane (PDMS) and 17.4 ppm (CH_3) of hexamethylbenzene (HMB) as external standards. Liquid-state ^{1}H and ^{29}Si NMR spectra were measured using a JEOL ECZ-500 spectrometer at a resonance frequency of 500.16 MHz (^{1}H) and 99.36 MHz (^{29}Si), a 45° pulse (Si), and a recycle delay of 5 s (^{1}H) and 10 s (^{29}Si). In a 5 mm glass sample tube, $CDCl_3$ was used as a deuterated solvent, and tetramethylsilane (TMS) was used as an internal standard with a chemical shift of 0 ppm. Fourier transform infrared (FT-IR) spectra were measured in KBr pellets using a FT/IR-6100 (JASCO) spectrometer. Microscopic Raman spectra were measured using an in-Via Reflex (Renishaw) spectrometer at an excitation wavelength of 532 nm. The contents of carbon, hydrogen, and nitrogen were measured using a CHN analysis instrument (PerkinElmer, 2400 Series II). The C, H, and N contents of some samples were analyzed using a Yanaco CHN corder Type MT-5. The temperatures of heating and oxidation (conc. 15% O_2) and the reduction furnaces were 950, 850, and 550 °C, respectively. The sulfur contents were analyzed by ion chromatography using an Organic Halogen/Sulfur Analysis System with a Yanaco SQ-10 instrument. Both chemical analyses were conducted by A-Rabbit-Science Japan Co. Ltd. The amounts of silicon and sodium were determined by inductively coupled plasma optical emission spectrometry (ICP-OES) (Agilent Technologies, Agilent 5100). A sample was prepared by a melting method using $Li_2B_4O_7$ as a flux. XPS spectra were measured with a PHI 5000 VersaProbe II (ULVAC-PHI, Inc.) spectrometer using AlKα. TEM images were obtained using a JEM-2010 (JEOL) microscope at an accelerating voltage of 200 kV, and HR-SEM images were obtained using an S-5500 microscope (Hitachi High-Technologies Co.) at an accelerating voltage of 1 kV.

Acknowledgements

We gratefully acknowledge Dr. M. Yoshikawa, Dr. N. Sato, Mr. Y. Shimasaki, Dr. T. Matsuno, Dr. K. Muramatsu, Mr. T. Hirohashi, Ms. R. Sakai, Mr. R. Suganami, Mr. Y. Oka, and Ms. A. Komatsu (Waseda University) for their assistance with sample preparation and fruitful discussions. We acknowledge Mr. S. Enomoto (Kagami Memorial Research Institute for Materials Science and Technology, Waseda University), Dr. T. Shibue, Dr. N. Sugimura, Mr. Y. Watabe (Material Characterization Central Laboratory, Waseda University[50]), and Ms. A. Kubota (Environmental Safety Center, Waseda University) for the XPS, NMR, and ICP analyses. Funding from the ANR (project ANR-15-JTIC-0003-01) to support the PhD scholarship of Dr. N. Rey is also gratefully acknowledged. This work was supported by grants Grant-in-Aid for Strategic International Collaborative Research Program (SICORP), the "France–Japan Joint Call On MOLECULAR TECHNOLOGY" from the ANR (Agence Nationale de la Recherche) and JST (Japan Science and Technology Agency) for the MODULE-CAT project (ANR-15-JTIC-0003-01) and JSPS for the Joint Research Projects-LEAD with DFG. M. K. is grateful for financial support via a Grant-in-Aid for JSPS Research Fellows from MEXT (No. 18J22738).

[1] N. Takahashi, K. Kuroda, *J. Mater. Chem.* **2011**, *21*, 14336–14353.
[2] E. Ruiz-Hitzky, P. Aranda, M. Darder, M. Ogawa, *Chem. Soc. Rev.* **2011**, *40*, 801–828.
[3] T. Okada, Y. Ide, M. Ogawa, *Chem. Asian J.* **2012**, *7*, 1980–1992.
[4] F. M. Fernandes, H. Baradari, C. Sanchez, *Appl. Clay Sci.* **2014**, *100*, 2–21.
[5] M. Faustini, L. Nicole, E. Ruiz-Hitzky, C. Sanchez, *Adv. Funct. Mater.* **2018**, *28*, 1704158.
[6] U. Díaz, A. Corma, *Chem. Eur. J.* **2018**, *24*, 3944–3958.
[7] N. Takahashi, H. Hata, K. Kuroda, *Chem. Mater.* **2010**, *22*, 3340–3348.
[8] Y. Ide, N. Kagawa, M. Sadakane, T. Sano, *Chem. Commun.* **2013**, *49*, 9027–9029.
[9] E. Doustkhah, S. Rostamnia, N. Tsunoji, J. Henzie, T. Takei, Y. Yamauchi, Y. Ide, *Chem. Commun.* **2018**, *54*, 4402–4405.
[10] D. Mochizuki, A. Shimojima, T. Imagawa, K. Kuroda, *J. Am. Chem. Soc.* **2005**, *127*, 7183–7191.
[11] Y. Asakura, Y. Matsuo, N. Takahashi, K. Kuroda, *Bull. Chem. Soc. Jpn.* **2011**, *84*, 968–975.
[12] N. Tsunoji, M. Bandyopadhyay, Y. Yagenji, H. Nishida, M. Sadakane, T. Sano, *Dalton Trans.* **2017**, *46*, 7441–7450.
[13] K. Isoda, K. Kuroda, M. Ogawa, *Chem. Mater.* **2000**, *12*, 1702–1707.
[14] R. Ishii, T. Ikeda, T. Ito, T. Ebina, T. Yokoyama, T. Hanaoka, F. Mizukami, *J. Mater. Chem.* **2006**, *16*, 4035–4043.
[15] U. Díaz, Á. Cantín, A. Corma, *Chem. Mater.* **2007**, *19*, 3686–3693.
[16] H. M. Moura, H. O. Pastore, *Dalton Trans.* **2014**, *43*, 10471–10483.
[17] S. Vortmann, J. Rius, S. Siegmann, H. Gies, *J. Phys. Chem. B* **1997**, *101*, 1292–1297.
[18] E. Ruiz-Hitzky, J. M. Rojo, *Nature* **1980**, *287*, 28–30.
[19] T. Yanagisawa, K. Kuroda, C. Kato, *React. Solids* **1988**, *5*, 167–175l.
[20] I. Fujita, K. Kuroda, M. Ogawa, *Chem. Mater.* **2005**, *17*, 3717–3722.
[21] K.-W. Park, J. H. Jung, S.-K. Kim, O.-Y. Kwon, *Appl. Clay Sci.* **2009**, *46*, 251–254.
[22] K.-W. Park, J. H. Jung, S.-K. Kim, O.-Y. Kwon, *Appl. Clay Sci.* **2004**, *27*, 21–27.
[23] C. J. Brinker, G. W. Scherer, *Sol-Gel Science: The Physics and Chemistry of Sol-Gel Processing*, Academic Press, Inc., San Diego, 1990, pp. 116–142.
[24] T. Montheil, C. Echalie, J. Martinez, G. Subra, A. Mehdi, *J. Mater. Chem. B* **2018**, *6*, 3434–3448.
[25] N. Rey, S. Carenco, C. Carcel, A. Ouali, D. Portehault, M. Wong Chi Man, C. Sanchez, *Eur. J. Inorg. Chem.* **2019**, *27*, 3148–3156.
[26] J–L. Bréfort, R. J. P. Corriu, C. Guérin, B. J. L. Henner, W. W. C. Wong Chi Man, *Organometallics* **1990**, *9*, 2082–2085.
[27] B. B. Kharkov, S. V. Dvinskikh, *J. Phys. Chem. C* **2013**, *117*, 24511–24517.
[28] C. Bisio, F. Carniato, G. Paul, G. Gatti, E. Boccaleri, L. Marchese, *Langmuir* **2011**, *27*, 7250–7257.
[29] Remaining TBAF could not be confirmed in both the ^{13}C CP/MAS NMR and FT-IR spectra, because the peaks overlap with other peaks.
[30] T. D. Courtney, C. C. Chang, R. J. Gorte, R. F. Lobo, W. Fan, V. Nikolakis, *Microporous Mesoporous Mater.* **2015**, *210*, 69–76.
[31] The amount of C arising from C_8TES was obtained by subtracting the amount of C arising from C_{16}TMA cation, which was calculated from the amount of nitrogen, from the total amount of carbon.
[32] T. Kimura, K. Kuroda, Y. Sugahara, K. Kuroda, *J. Porous Mater.* **1998**, *5*, 127–132.
[33] Y. Mitamura, Y. Komori, S. Hayashi, Y. Sugahara, K. Kuroda, *Chem. Mater.* **2001**, *13*, 3747–3753.
[34] The XPS peak arising from F 1s at 685 eV is attributed to fluoride species possibly located in the interlayer space.
[35] J. Pereira, L. E. Pichon, R. Dussart, C. Cardinaud, C. Y. Duluard, E. H. Oubensaid, P. Lefaucheux, M. Bounfichel, P. Ranson, *Appl. Phys. Lett.* **2009**, *94*, 07501–1–07501–3.
[36] F^- may attack Si atoms of octosilicate. However, it is difficult to quantitatively estimate how much F^- attacks the silicon atoms.
[37] D. Mochizuki, S. Kowata, K. Kuroda, *Chem. Mater.* **2006**, *18*, 5223–5229.
[38] J. Alauzun, A. Mehdi, C. Reyé, R. J. P. Corriu, *Chem. Commun.* **2006**, 347–349.
[39] Y. Ide, G. Ozaki, M. Ogawa, *Langmuir* **2009**, *25*, 5276–5281.
[40] Y. S. Li, Y. Wang, A. Perkins, *Spectrochim. Acta Part A* **2005**, *61*, 3032–3037.
[41] J. Li, D. Cheng, T. Yin, W. Chen, Y. Lin, J. Chen, R. Li, X. Shuai, *Nanoscale* **2014**, *6*, 1732–1740.
[42] The carbon contents in MP-Oct and MP-Oct_0.27F were not corrected by considering the carbon content of remaining C_{16}TMA cations because the amounts of N for both of the cases were very small.
[43] When all silylated sites are grafted with 3-mercaptopropyl*monoethoxy*silyl groups (ie. ethoxy groups are not hydrolyzed), the ratio of C/S is calculated to be 5. When all silylated sites are grafted with 3-mercaptopropyl*hydroxy*silyl groups (ie. all ethoxy groups are hydrolyzed), the ratio of C/S is 3.
[44] P. Moriones, G. Arzamendi, J. J. Garrido, J. C. Echeverria, *J. Phys. Chem. A* **2019**, *123*, 10364–10371.
[45] M. C. B. Salon, P. A. Bayle, M. Abdelmouleh, S. Boufi, M. N. Belgacem, *Colloids Surf. A* **2008**, *312*, 83–91.
[46] A. P. Amrute, B. Zibrowius, F. Schüth, *Chem. Mater.* **2020**, *32*, 4699–4706.
[47] L. Chmielarz, P. Kuśtrowski, R. Dziembaj, P. Cool, E. F. Vansant, *Microporous Mesoporous Mater.* **2010**, *127*, 133–141.
[48] D. Zhao, J. Feng, Q. Huo, N. Melosh, G. H. Frederickson, B. F. Chmelka, G. D. Stucky, *Science* **1998**, *279*, 548–552.
[49] As a reference experiment, silylation without TBAF but in the presence of THF in addition to DMF was conducted. The degree of silylation was calculated to be 48%, and the value is in the mid of degrees of silylation for C_8-Oct (33%) and C_8-Oct_0.27F (60%). Thus, THF also affects the degree of silylation to some extent, though the details have not been investigated yet.
[50] C. Izutani, D. Fukagawa, M. Miyasita, M. Ito, N. Sugimura, R. Aoyama, T. Gotoh, T. Shibue, Y. Igarashi, H. Oshio, *J. Chem. Educ.* **2016**, *93*, 1667–1670.

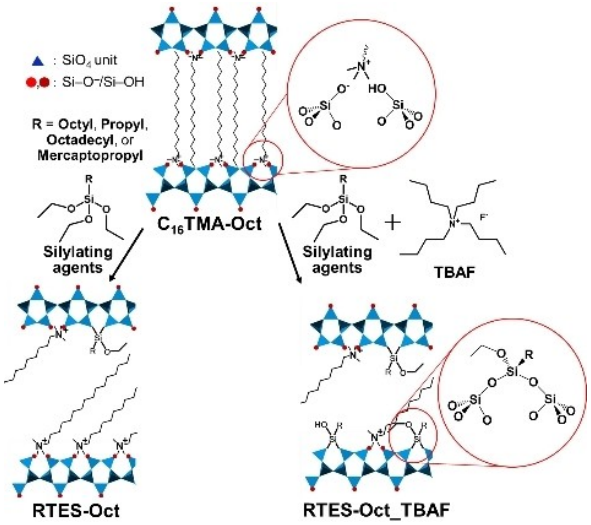

Interlayer silylation of layered octosili-cate with organotriethoxysilane was enhanced by the addition of TBAF. The F^- in TBAF attacks the silicon in alkoxysilanes, which increases the re-activity with SiOH groups on the layer surface. The effect of F on silylation depends on the kind of functional organic group of organotrieth-oxysilanes, because the interlayer ac-cessibility is varied with functional groups.